Available online at www.sciencedirect.com
ScienceDirect
Surface Science 602 (2008) 1607–1613
SURFACE SCIENCE
www.elsevier.com/locate/susc

Scanning probe microscopy study of exfoliated oxidized graphene sheets

D. Pandey [a,b,*], R. Reifenberger [a,b], R. Piner [c]

[a] Department of Physics, Purdue University, West Lafayette, IN 47907, United States
[b] Brick Nanotechnology Center, Purdue University, West Lafayette, IN 47907, United States
[c] Department of Mechanical Engineering, The University of Texas at Austin, Austin, TX 78712-0292, United States

Received 15 November 2007; accepted for publication 4 February 2008
Available online 23 February 2008

Abstract

Exfoliated oxidized graphene (OG) sheets, suspended in an aqueous solution, were deposited on freshly cleaved HOPG and studied by ambient AFM and UHV STM. The AFM images revealed oxidized graphene sheets with a lateral dimension of ~5–10 μm. The oxidized graphene sheets exhibited different thicknesses and were found to conformally coat the HOPG substrate. Wrinkles and folds induced by the deposition process were clearly observed. Phase imaging and lateral force microscopy showed distinct contrast between the oxidized graphene and the underlying HOPG substrate. The UHV STM studies of oxidized graphene revealed atomic scale periodicity showing a (0.273 ± 0.008) nm $\times$ (0.406 ± 0.013) nm unit cell over distances spanning few nanometers. This periodicity is identified with oxygen atoms bound to the oxidized graphene sheet. $I(V)$ data were taken from oxidized graphene sheets and compared to similar data obtained from bulk HOPG. The dI/dV data from oxidized graphene reveals a reduction in the local density of states for bias voltages in the range of ± 0.1 V.
Published by Elsevier B.V.

Keywords: Atomic force microscopy; Lateral force microscopy; Scanning tunneling microscopy; Scanning tunneling spectroscopy; Highly oriented pyrolitic graphite; Oxidized graphene (OG)

1. Introduction

Graphene, an aromatic-based substance which is a 2-D counterpart of 3-D graphite, could well be one of the prominent new materials for next generation nanoelectronic devices. Graphene is a single planer sheet, ~0.5 nm thick, formed from sp^2 bonded carbon atoms. Calculations assuming 1-D ribbons of graphene demonstrate unique electrical properties that suggest either metallic or semiconducting behavior can be achieved [1]. Recently, experiments on suspended graphene sheets suggest long range crystalline order in addition to out-of-plane surface corrugation [2]. From a device perspective, ultra thin graphene sheets have reportedly been grown on single crystal silicon carbide by vacuum graphitization and the graphene sheets were patterned by a standard nanolithographic method [3]. By chemical modification of graphite, soluble fragments of graphene can be prepared in the laboratory [4]. Transistors have also been created using a single sheet of graphene [5].

A required component for the future development of a graphene-based electronics is a stable oxide, somewhat analogous to the widespread use of $Si–SiO_2$ in the microelectronics industry. It is a fair question whether the electronic properties of oxidized graphene are suitable to form the equivalent of insulating oxidized silicon layers. If oxidized graphene can be used in conjunction with graphene sheets, then a viable manufacturing technology for the fabrication of future nanoelectronic devices might emerge.

* Corresponding author. Address: Department of Physics, Purdue University, West Lafayette, IN 47907, United States. Tel.: +1 765 4965211.
E-mail address: dpandey@physics.purdue.edu (D. Pandey).

0039-6028/$ - see front matter Published by Elsevier B.V.
doi:10.1016/j.susc.2008.02.025

Evidently, oxidized graphite was prepared circa 1860 by oxidizing graphite using $KClO_3$ and HNO_3 [6]. The resulting material is nonstoichiometric. Subsequently, various models were proposed to understand the atomic structure of oxidized graphite [7,8]. NMR and XPS studies suggest that oxygen functional groups attach to the carbon atoms in the basal plane. Recently, oxidized graphite has been used to make a new layered material called graphene oxide paper [9]. This new material is comprised of individual hydrophilic oxygenated graphene sheets.

In spite of the recent interest in graphene, little is known about the atomic structure and electronic properties of oxidized graphene. A few studies conducted under ambient conditions have been performed to study oxidized graphite [10,11]. Recent work has measured the temperature dependence of the conductivity of oxidized graphene sheets of varying thickness [12]. In what follows below, we report on our efforts to better characterize oxidized graphene sheets deposited onto HOPG substrates. In this initial study, both UHV STM and ambient AFM techniques were chosen because they provide reliable topographic and electronic information with atomic scale resolution.

2. Sample preparation

2.1. Synthesis and characterization of oxidized graphene sheets

The oxidized graphene used in this study was synthesized from purified natural graphite (SP-1, Bay carbon) by the Hummers method [13]. Briefly, it has been shown that oxidized graphene can undergo complete exfoliation in water, providing individual oxidized graphene sheets. Following purification and filtering, these oxidized graphene sheets are suspended in water by stirring (no sonication), forming a clear liquid suitable for deposition on a substrate of choice. Flakes having typical lateral dimension of ~5–10 μm were routinely observed. These flakes are ~5–10 times larger than previously reported [14,15]. Prior to study by scanning probe techniques, thick layers of the oxidized graphene sheets were formed and characterized using an optical microscope, which shows the color of the deposited material under transmitted white light is dark brown and black in reflection [9].

2.2. Preparation of oxidized graphene sample and HOPG reference sample

A 1 cm × 1 cm substrate of highly-oriented pyrolitic graphite (HOPG) was prepared by first cleaving the HOPG surface with adhesive tape. A 2 μL drop of a solution containing oxidized graphene sheets suspended in ultra pure water was deposited on the freshly cleaved HOPG substrate. After deposition, the drop covered the entire 1 cm^2 area of the HOPG substrate. The HOPG was then placed in a covered Petri dish for approximately 3 h to allow the oxidized graphene sheets to adhere to the HOPG surface. After 3 h, the excess solution was removed from the HOPG using lint free tissue paper to rapidly remove any salt or impurity present in the solution. This procedure was adopted rather than complete evaporation of the solution to reduce any impurities which might settle onto the oxidized graphene sheets.

A second 1 cm^2 substrate of HOPG was prepared by cleaving the surface with adhesive tape. This second (reference) substrate allowed a ready comparison of results obtained from the oxidized graphene sample.

3. Experimental considerations

Two experimental set-ups were used for the investigations. The STM/STS experiments were performed by an Omicron UHV STM with three compartmentalize chambers serving as a sample insertion chamber, a sample processing chamber and an STM chamber. The STM is housed in a vacuum chamber with a base pressure better than 8×10^{-10} Torr. The STM apparatus is in a shielded room and is resting on a vibration isolation concrete slab situated in the Birck Nanotechnology Center, Purdue University.

The tip used in the STM/STS study was made of W and was etched by the dc drop-off method [16,17]. The aqueous solution used was 2 M NaOH. The etching voltage was 12 V. In this set-up, the cathode was a carbon rod and the anode was the W wire.

After inserting into the vacuum chamber, the tip was annealed by a bare filament for ~5 min before scanning. The gap (bias) voltage is applied to the sample with respect to the tip which is at ground potential. The STM scans were limited to areas of 500 nm × 500 nm or less.

Topography and phase contrast AFM data were obtained under ambient conditions using a Park Systems model XE-100. The images shown were made in noncontact mode, with a silicon tip using a scanning speed of ~0.5 Hz. The resonance frequency of the microcantilever was approximately 300 kHz. The AFM scans were generally limited to areas of 10 μm × 10 μm or less.

Lateral force measurements (LFM) were performed using a Park Scientific model CP AFM. The LFM images were recorded in contact mode with a normal force set point of ~1 nN.

4. Result and discussion

4.1. AFM study of oxidized graphene sheets on HOPG

An extensive AFM study was performed to characterize the oxidized graphene sheets deposited onto the HOPG surface. The conclusions from this AFM study are summarized as follows.

There is clear evidence of deposited oxidized graphene sheets on a freshly cleaved HOPG surface. The AFM images reveal a complex morphology that depends somewhat on the deposition conditions. As an example, when an oxidized graphene sheet is deposited onto clean HOPG,

it exhibits regions that conformally bind to the HOPG surface as well as regions that wrinkle and fold back onto itself. Similar structures have been observed in the earliest electron micrographs of graphite oxide [18]. In topographic images of the folds, the oxidized graphene sheets appear to have a thickness restricted to integer multiples of ~0.67 nm. This should be compared to values of 0.65–0.75 nm reported for the intergraphene spacing of graphite oxide, [19] and the value of 1.1 ± 0.2 nm reported for deposited oxidized graphene sheets on SiO_2 [12].

The wrinkles appear as 1-dimensional ridges that form due to the non-planar deposition of an oxidized graphene sheet on to the HOPG substrate. The wrinkles are more prevalent as the size of the oxidized graphene sheet increases. The wrinkles have variable heights that are approximately 1.0–4.5 nm above the oxidized graphene sheet.

An illustration of these above observations are given in Fig. 1a which shows a typical large area AFM scan of the oxidized graphene sample. The image illustrates flat regions that conform to the underlying substrate plus evidence for wrinkles and folds. Clear atomic scale steps in the underlying HOPG substrate are evident. These steps are decorated by nanometer scale particulates of unknown composition. Fig. 1b is a magnified image from a selected region in Fig. 1a that illustrates the folding of oxidized graphene as well as two prominent wrinkles.

The folding morphology was investigated in more detail by making a histogram of the z heights from the boxed region outlined in Fig. 1b and is given in Fig. 1c. The histogram shows the HOPG substrate (distributed about a height of 0 nm) plus evidence for multilayer of oxidized graphene sheets that are integer multiples of a layer height $h \cong 0.67$ nm. Similar features attributed to wrinkles and

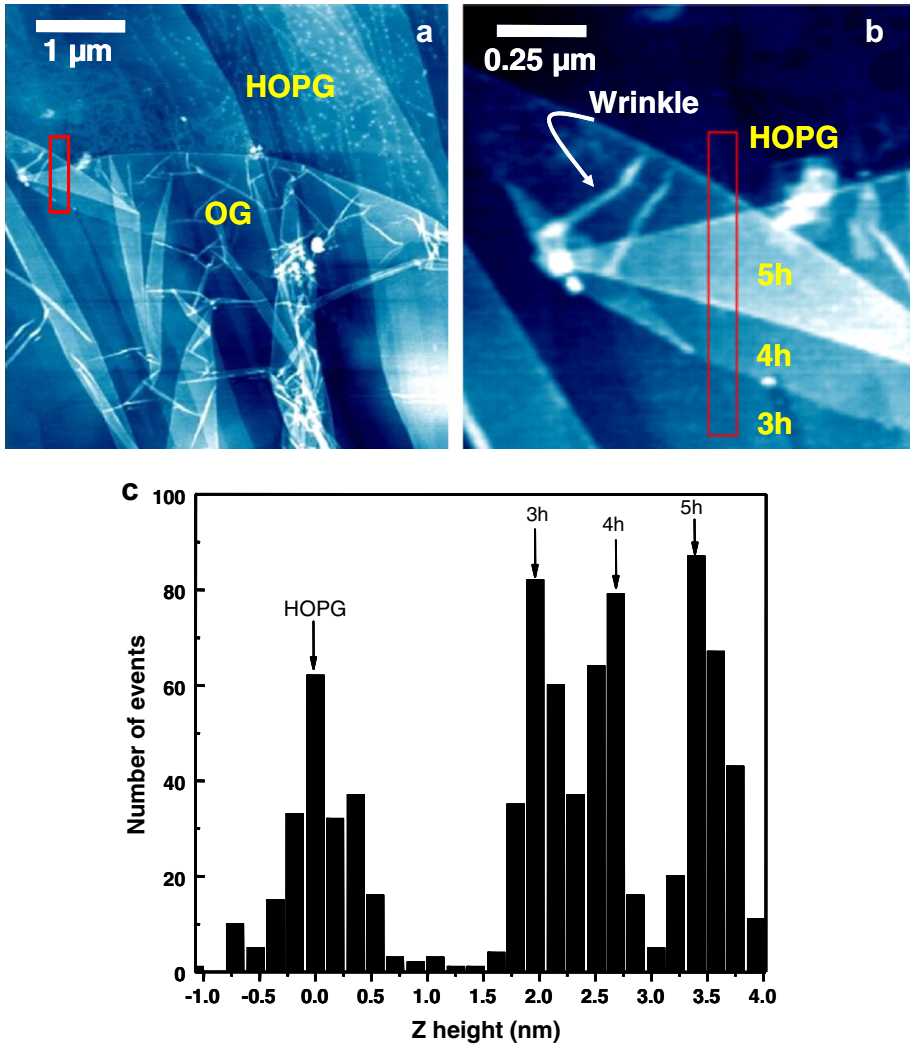

Fig. 1. Typical non-contact topographic image of oxidized graphene on an HOPG substrate obtained by AFM. Prominent wrinkling, presumably related to the deposition of oxidized graphene, is observed. In (a), an image of a 5×5 μm^2 oxidized graphene sample. In (b), a magnified image illustrating folds and wrinkles in the deposited oxidized graphene sheet. In (c), a z-height histogram of the boxed region of the AFM image in (b) shows the presence of integer layers of an oxidized graphene sheet. From the data, a value for the height h of one layer of an oxidized graphene sheet is inferred to be $h \cong 0.67$ nm.

folds, albeit at a more magnified scale, were also observed during our studies with STM.

We also undertook experiments to determine if the chemical difference between oxidized graphene and the underlying HOPG substrate can be resolved. As shown in Fig. 2, both phase and lateral force images reveal a contrast related to the different chemical composition of the two materials under study. Fig 2a clearly shows an overall phase contrast between oxidized graphene and HOPG. In addition, the phase image also shows enhanced contrast of wrinkles (in oxidized graphene) and step edges (in HOPG), presumably due to controller error. Fig. 2b shows a typical LFM image of an oxidized graphene flake on HOPG and provides clear contrast between the two surfaces, indicating a difference in friction between the two different materials. In this LFM image, higher friction is shown as a brighter color. Topography and lateral force images taken at the same spot indicates that the friction is higher on the oxidized graphene surface than on HOPG.

4.2. STM study of oxidized graphene sheets on HOPG

4.2.1. STM topography

Extensive STM studies were performed on different samples of clean HOPG and oxidized graphene. The studies ranged from routine STM imaging to careful measurements of $I(V)$. The same dc-etched W tip was used in all STM studies. Typical large area ($500 \times 500\ \mathrm{nm}^2$) STM images revealed features similar to those observed in the AFM studies discussed above. In addition, atomic resolution was obtained on clean HOPG as well as on oxidized graphene sheets deposited on HOPG at small scale. The atomically resolved HOPG images were used to calibrate the X–Y piezo used in this study. The STM images were analyzed using WSxM, version 7.3 [20].

As shown in Fig. 3, a typical STM topographic image of an oxidized graphene sheet taken at higher spatial resolution than possible with AFM reveals features that are very similar to the topographic images obtained during the

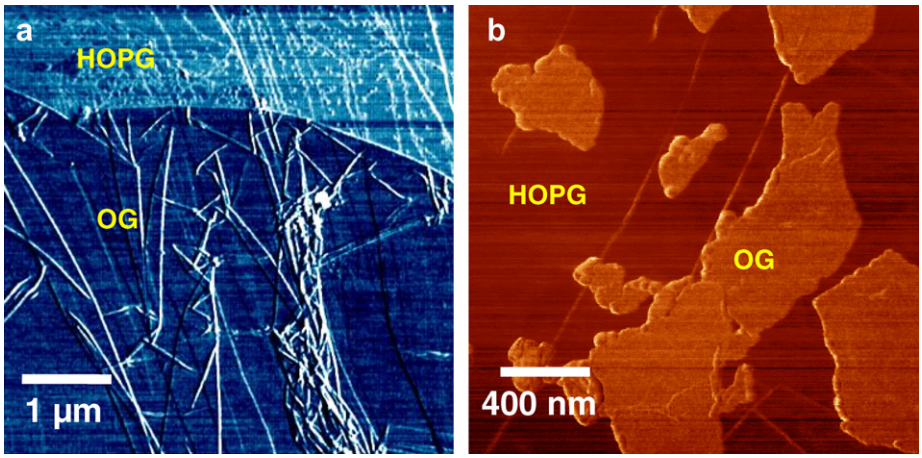

Fig. 2. Typical phase and lateral force images of oxidized graphene deposited on an HOPG substrate. (a) The phase contrast image of oxidized graphene on HOPG (same region shown in Fig. 1a) clearly shows a boundary between the HOPG substrate and the oxidized graphene sheet. In (b), a lateral force image of oxidized graphene flakes on HOPG clearly indicates a difference between the lateral forces on HOPG and oxidized graphene. Both images indicate a clear chemical difference between the HOPG substrate and the oxidized graphene sheet.

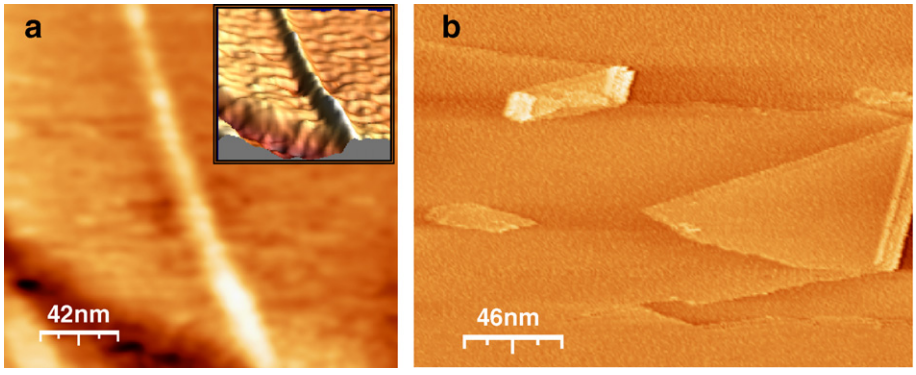

Fig. 3. Typical topographic images of oxidized graphene sheets deposited on an HOPG substrate obtained by UHV STM. In (a), a topographic image illustrating a wrinkle formed in an oxidized graphene sheet. The feature increases in width and is ~1 nm high. The inset provides a 3-dimensional rendering of the feature. In (b), a topographic image illustrating a fold in an oxidized graphene sheet. The folded edge (visible in the rightmost edge of the image) exhibits a sequence of three closely-spaced parallel features that form to relax the stress that develops when the sheet folds.

AFM study. In Fig. 3a, the 1-dimensional feature observed in the STM image is attributed to a wrinkle in the middle of an oxidized graphene sheet. The feature increases in width in much the same way as a ruck forms when a flexible cloth is dropped onto a rigid substrate. From Fig. 3, the height of this feature is approximately 1 nm. Fig. 3b shows a typical image of a portion of an oxidized graphene sheet that has folded onto itself. The folded edge exhibits a sequence of parallel features that form to relieve the stress.

4.2.2. Atomically resolved STM studies

Atomically resolved, constant height images of clean HOPG taken under UHV conditions were performed to calibrate the piezo scanner for nanometer-sized scales. The atomic features were organized in a hexagonal pattern with an atom spacing of 0.25 nm [21]. The periodicity of the features was independent of scan rate and bias voltage.

Similar constant height studies were performed on an oxidized graphene sheet as shown in Fig. 4 which reveals that the oxidized graphene surface has a rectangular lattice. The lattice constants were statistically estimated by independently measuring the spacing between adjacent features. This analysis provides an unbiased estimate for the mean lattice constant and provides a realistic estimate for the standard deviation from the mean. In this way, lattice constants of (0.273 ± 0.008) nm $\times$ (0.406 ± 0.013) nm were determined. This atomically resolved structure was not observed at all locations on the oxidized graphene sheet. It was seen in ~50% of the high resolution STM scans performed. In the remaining scans, no recognizable atomic scale periodicity was observed. We also note that for atomic-scale imaging (scans less than ~3 nm), a tip bias exceeding ~300 mV caused excessive noise in the tunnel current and prevented reliable imaging.

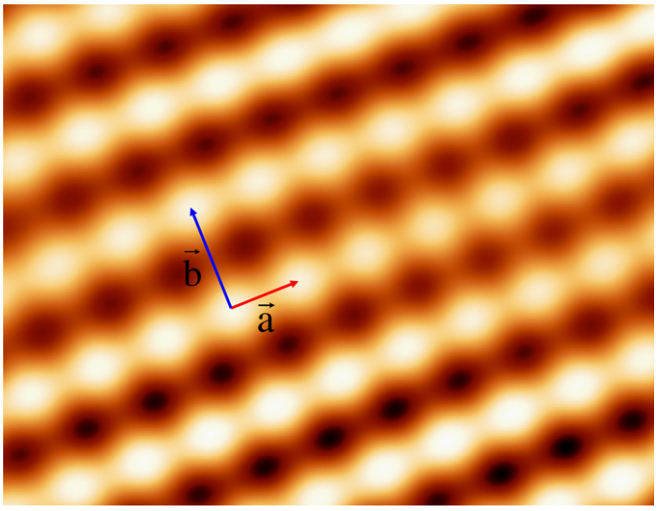

Fig. 4. High resolution UHV STM image of oxidized graphene lattice revealing a rectangular lattice. From a statistical analysis, $\vec{a} = (0.273 \pm 0.008)$ nm; $\vec{b} = (0.406 \pm 0.013)$ nm. Tip bias: +100 mV; tunneling current 0.5 nA.

The atomic structure of graphite oxide has been studied for over 70 years. In the 1930's, Hoffmann et al., proposed a structure in which the O atoms in graphite oxide are bound to the C atoms in the basal plane [7,8]. From early work, there was evidence that hydroxyl atoms are also present in graphite oxide [8,22]. Further work suggested the presence of carboxylic groups on the periphery of graphite oxide [23,24]. Solid state ^{13}C NMR studies provided evidence for C–OH, C–O–C, and >C=C< groups in graphite oxide [25,26]. Klusek used both XPS and STM to study the surface of oxidized HOPG. Using XPS, he found evidence for O and carboxylic groups on the surface. No atomic resolution was achieved from the STM studies [10].

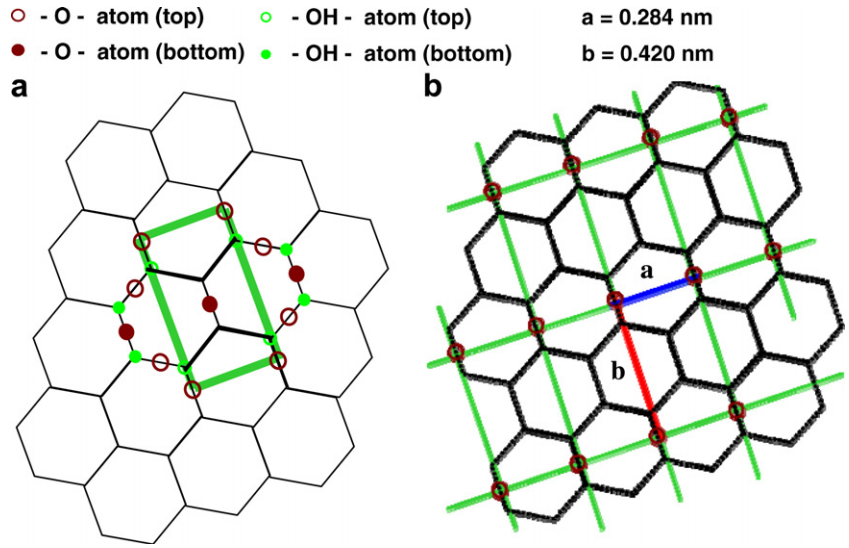

Fig. 5. Schematic diagram representing the possible position of functional groups bonded to carbon atoms, with in one oxidized graphene layer. Carbon atoms are positioned at each corner of the hexagon. In (a), the brown (hollow and solid) circles represent the possible position of –CO group and the green (hollow and solid) circles represents the possible position of –OH group. In (b), the expected rectangular unit cell formed by O atoms on a graphene sheet. From Ref. [26].

Recently, a model for the bonding sites of –O and –OH to a graphene layer was published [27]. This model, reproduced in Fig. 5, can be used to understand the atomically resolved STM images obtained in our study.

The model in Fig. 5a shows the possible positions of –O and –OH groups bonded to the top and bottom of a graphene sheet to form oxidized graphene. Since graphite oxide is non-stoichiometric, a layer of oxidized graphene may contain a random arrangement of these oxygen-containing groups. To understand the atomically resolved STM image in Fig. 4, it is useful to focus attention on the position of oxygen on the top of the graphene sheet. A unit cell comprising the O atoms is sketched in Fig. 5b.

From the known size of the graphite lattice, we estimate the size of the unit cell for the O lattice pictured in Fig. 5b to be 0.284 nm by 0.420 nm. This agrees well with the observed periodicity of (0.273 ± 0.008) nm $\times$ (0.406 ± 0.013) nm from the atomically resolved STM image shown in Fig. 4. The atomically resolved lattice structure is not observed at all regions across the oxidized graphene sample, leading to the conclusion that other regions may contain hydroxyl and carboxylic groups.

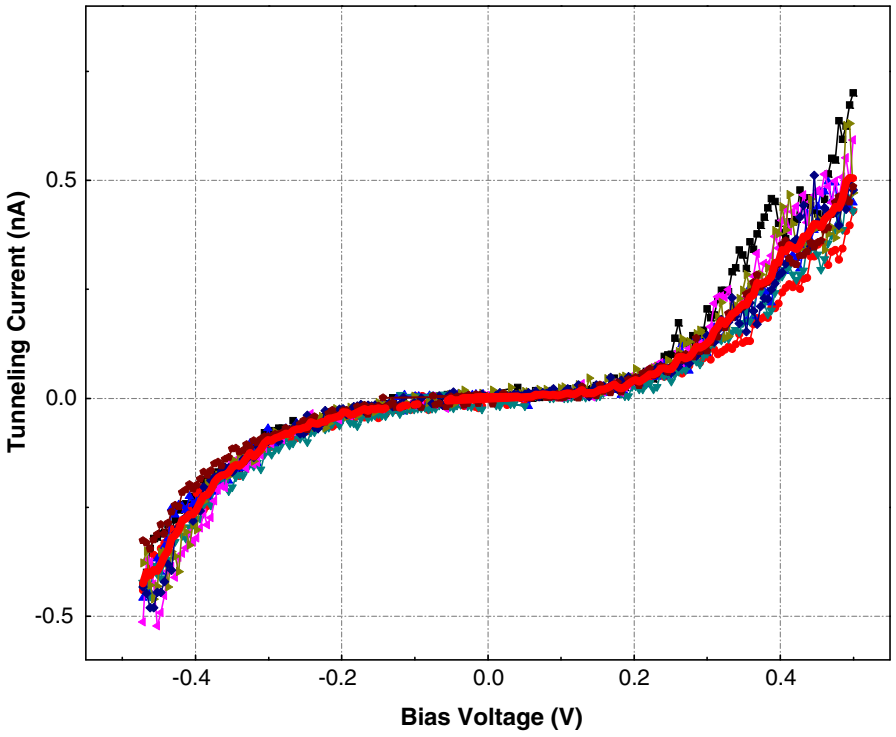

Fig. 6. Typical $I(V)$ data from oxidized graphene illustrating reproducibility across a 2.5 nm x 2.5 nm region at 10 different (x, y) points. $I_{set} = -0.5$ nA; $V_{set} = -0.5$ V.

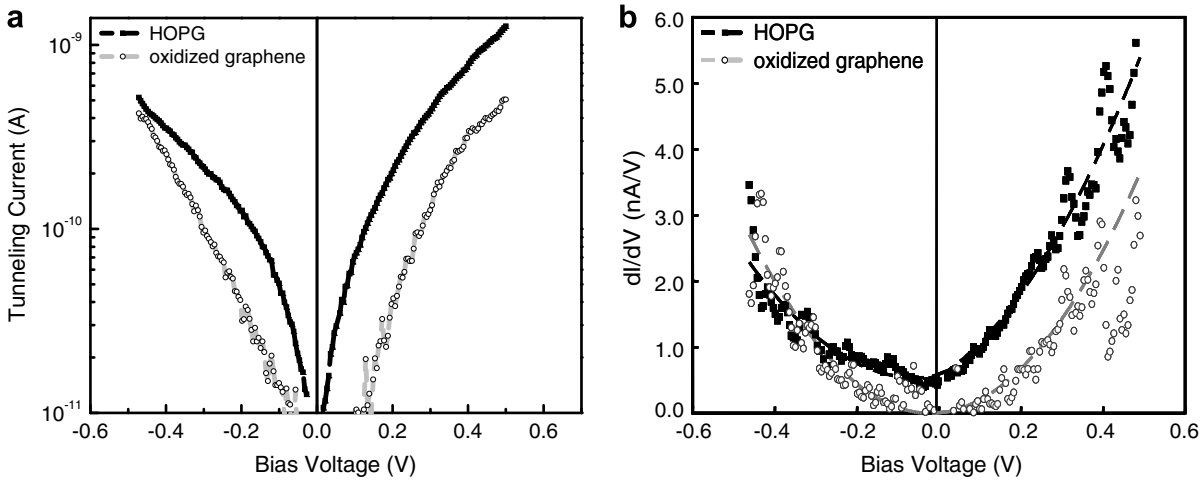

Fig. 7. Representative $I(V)$ and dI/dV data for HOPG and oxidized graphene on HOPG. The dashed lines through the dI/dV data are drawn as guides to the eye.

4.2.3. STS of oxidized graphene

We have also established that reproducible $I(V)$ spectra could be acquired from both HOPG and oxidized graphene. The $I(V)$ data were taken by first maintaining a specified set point current ($-I_{set}$) with the tip biased to a specified value ($-V_{set}$). Typical values are $I_{set} = -0.5$ nA or -1.0 nA; $V_{set} = -0.5$ V, -1.0 V, and -1.5 V. The feedback was then disabled and 200 data points were acquired as the voltage was ramped from $-V_{set}$ to $+V_{set}$. After completion of the voltage sweep, the feedback was once again enabled to establish the initial conditions. Typically, this procedure was repeated to acquire $I(V)$ data at ten different (x, y) positions within a 2.5 nm × 2.5 nm region similar to that shown in Fig. 4.

The $I(V)$ data obtained in this way from either oxidized graphene or HOPG was reproducible as is demonstrated in Fig. 6 for the case of oxidized graphene.

Fig. 7 compares an average $I(V)$ and dI/dV for both HOPG and oxidized graphene. Derivatives of the averaged $I(V)$ data were performed by first applying a 5-point smoothing algorithm to the $I(V)$ data and then calculating the derivative numerically. From the $I(V)$ data, a clear suppression of current near zero bias is observed for the case of oxidized graphene. Since dI/dV at low bias is proportional to the local density of electronic states (LDOS), the dI/dV data indicate a measurable suppression in the LDOS for oxidized graphene that extends ±0.1 V about zero bias. From Fig. 7a which plots $\log_{10}[|I|]$ vs. V_{bias}, evidence for a bandgap in oxidized graphene of ~0.25 eV can be inferred.

5. Conclusions

The results of a scanning probe microscope study on oxidized graphene sheets have been described. Ambient AFM shows that the oxidized graphene sheets conformally coat an HOPG substrate. Wrinkles and folds in the oxidized graphene sheet are clearly observed. The UHV STM study has resolved the atomic lattice of an oxidized graphene sheet deposited onto HOPG. High resolution STM images indicate that regions of oxidized graphene form an ordered, rectangular array of atoms with a periodicity of (0.273 ± 0.008) nm × (0.406 ± 0.013) nm. We attribute this atomic periodicity to the O atoms that are bound to the graphene sheet. STM $I(V)$ data show a lower conductivity for oxidized graphene for all tip-substrate separations studied. Under low tip bias conditions, the STM-oxidized graphene tunnel junction exhibits a conductance that is ~10 times smaller than that observed for HOPG under similar conditions. Evidence for a bandgap in oxidized graphene of ~0.25 eV can be inferred.

Acknowledgements

The exfoliated oxidized graphene sheets were prepared by Sasha Stankovich working in the laboratory of Rodney Ruoff at Northwestern University. This work was supported by NASA (Award # NCC-1-02037) through the University Research, Engineering and Technology Institute (URETI) on Bio-inspired Materials (BiMat).

References

[1] S. Philip, Z. Yiming, M. Mitch, M.A. Pulickel, K.N. Saroj, Appl. Phys. Lett. 91 (2007) 042101.
[2] J.C. Meyer, A.K. Geim, M.I. Katsnelson, K.S. Novoselov, T.J. Booth, S. Roth, Nature 446 (2007) 60.
[3] C. Berger et al., Science 312 (2006) 1191.
[4] S. Niyogi, E. Bekyarova, M.E. Itkis, J.L. McWilliams, M.A. Hamon, R.C. Haddon, J. Am. Chem. Soc. 128 (2006) 7720.
[5] A.K. Geim, K.S. Novoselov, Nature Mater. 6 (2007) 183.
[6] M.B.C. Brodie, Ann. Chim. Phys. 59 (1860) 466.
[7] U. Hofmann, A. Frenzel, E. Csalan, Liebigs Ann. Chem. 510 (1934).
[8] U. Hofmann, R. Holst, Ber. Dtsch. Chem. Ges. 72 (1939) 754.
[9] D.A. Dikin, S. Stankovich, E.J. Zimney, R.D. Piner, G.H.B. Dommett, G. Evmenenko, S.T. Nguyen, R.S. Ruoff, Nature 448 (2007) 457.
[10] Z. Klusek, Appl. Surf. Sci. 108 (1997) 405.
[11] Z. Klusek, P.K. Datta, W. Kozlowski, Corros. Sci. 45 (2003) 1383.
[12] C. Gomez-Navarro, R.T. Weitz, A.M. Bittner, M. Scolari, A. Mews, M. Burghard, K. Kern, Nano Lett. (2007).
[13] W.S. Hummers, R.E. Offeman, J. Am. Chem. Soc. 80 (1958) 1339.
[14] S. Stankovich, R.D. Piner, X.Q. Chen, N.Q. Wu, S.T. Nguyen, R.S. Ruoff, J. Mater. Chem. 16 (2006) 155.
[15] S. Stankovich, D.A. Dikin, G.H.B. Dommett, K.M. Kohlhaas, E.J. Zimney, E.A. Stach, R.D. Piner, S.T. Nguyen, R.S. Ruoff, Nature 442 (2006) 282.
[16] A.J. Melmed, The Art and Science and Other Aspects of Making Sharp Tips, AVS, Boston, MA, USA, 1991.
[17] J. Mendez, M. Luna, A.M. Baro, Surf. Sci. 266 (1992) 294.
[18] R.J. Beckett, R.C. Croft, J. Phys. Chem. 56 (1952) 929.
[19] H.C. Schniepp, J.L. Li, M.J. McAllister, H. Sai, M. Herrera-Alonso, D.H. Adamson, R.K. Prud'homme, R. Car, D.A. Saville, I.A. Aksay, J. Phys. Chem. B 110 (2006) 8535.
[20] I. Horcas, R. Fernandez, J.M. Gomez-Rodriguez, J. Colchero, J. Gomez-Herrero, A.M. Baro, Rev. Sci. Instrum. 78 (2007) 013705.
[21] H.A. Mizes, S.-i. Park, W.A. Harrison, Phys. Rev. B 36 (1987) 4491.
[22] J. Weiss, Nature 114 (1940) 744.
[23] A. Clauss, R. Plass, H.P. Boehm, U. Hofmann, Z. Anorg. Allg. Chem. 291 (1957) 205.
[24] W. Scholz, H.P. Boehm, Z. Anorg. U. Allgem. Chem. 369 (1969).
[25] H. He, T. Riedl, A. Lerf, J. Klinowski, J. Phys. Chem. 100 (1996) 19954.
[26] A. Lerf, H. He, M. Forster, J. Klinowski, J. Phys. Chem. B 102 (1998) 4477.
[27] A. Buchsteiner, A. Lerf, J. Pieper, J. Phys. Chem. B 110 (2006) 22328.